PHYSICAL REVIEW B VOLUME 12, NUMBER 11 1 DECEMBER 1975

Electronic Raman spectra of divalent cobalt ions in cadmium-chloride–type crystals*

J. C. Christie, I. W. Johnstone, G. D. Jones, and K. Zdansky†
Department of Physics, University of Canterbury, Christchurch, New Zealand
(Received 18 February 1975)

The polarized Raman spectra of divalent cobalt ions at concentrations ranging from 2.5 to 10 wt% in cadmium chloride, cadmium bromide, manganese chloride, and cobalt chloride from 15 to 300°K are reported. All five electronic transitions between the spin-orbit and trigonal crystal-field-split levels of the $^4T_{1g}(^4F)$ cubic-field ground term are observed with frequencies of 235, 499, 923, 953, and 1088 cm^{-1} for cadmium-chloride crystals containing 2.5-wt% cobalt. The strong-field matrices of the trigonal crystal field and the Zeeman interaction are calculated and quantitatively explain the experimental data. The d^3 configuration parameter values for the cadmium-chloride crystals with 2.5-wt% cobalt are (in cm^{-1}) $Dq = -670$, $B = 790$, $C = 3320$, $\zeta = -512$, $\zeta' = -513$, $v = 57$, and $v' = -345$. EPR measurements on the cadimum-bromide crystals with 0.1-wt% cobalt yield new values of $g_\parallel = 3.74 \pm 0.1$ and $g_\perp = 4.67 \pm 0.1$ which resolve difficulties in fitting the experimental data for this crystal. Raman lines were also observed for antiferromagnetically ordered $CoCl_2$.

I. INTRODUCTION

The energy levels of the $3d^7$ configuration characterize the electronic spectra of divalent cobalt ions. Those below 2000 cm^{-1} may be observed by infrared absorption or by electronic-Raman-scattering measurements with suitable crystals.

In this paper we report Raman-scattering measurements for crystals of cadmium chloride, cadmium bromide, and manganese chloride containing cobalt and for cobalt chloride.

Cadmium-chloride-type crystals were chosen as hosts for these studies because of the following reasons:

(i) The metal cations are located in sites which have only a slight trigonal distortion from cubic symmetry.

(ii) Cadmium chloride, cadmium bromide, manganese chloride, and cobalt chloride are all isomorphic and spectral changes caused by the variation of either the cation or anion in a given crystal structure can be readily investigated.

(iii) The $\vec{k} = 0$ lattice phonon spectra of all four crystals have been previously determined by infrared-absorption[1] and Raman-scattering measurements.[2]

(iv) The crystals containing cobalt are generally blue colored and can be examined with argon-ion laser excitation with the possibility of resonance enhancement.

(v) The cobalt-ion concentration may be varied over a wide range to distinguish the spectra of both single cobalt ions and of cobalt-ion clusters. Cobalt chloride itself becomes antiferromagnetically ordered below 24.71°K and the effects of such magnetic ordering on the spectra can also be determined.

In this paper, the Raman spectra observed are described in Sec. III. The Raman spectra of single cobalt ions are analyzed in Sec. IV B using a crystal-field model involving all 120 states of the $3d^7$ configuration. Parameters describing the trigonal crystal field and the spin-orbit interaction are obtained.

Several papers have reported preliminary investigations of the electronic Raman spectra of these crystals.[2-4] This paper presents some new experimental results, including polarization of some of the electronic Raman lines, and contains the first detailed crystal-field analysis of the spectra.

II. EXPERIMENTAL

All the crystals are hygroscopic and care must be taken in their preparation and mounting in order to prevent contamination by moisture. The crystals were grown from the melt by the Stockbarger method. Analar grade powders of the hydrated salts were first dehydrated by heating at 200 °C under vacuum for several days. They were purified of oxide and residual water by passing dry hydrogen chloride or hydrogen bromide (as appropriate) through the materials for several hours as they were being heated to the melting point and then bubbling the gas through the melt for an additional hour. The purified melt was filtered through a sintered quartz sieve into a quartz tube which was sealed off. The crystals were grown by slowly lowering the sealed quartz ampoule through a sharp temperature gradient. The resulting crystal boules were typically of dimension 8-mm diam by 20-mm long, and comprised a single crystal if the tip of the ampoule was shaped to allow the growth of only one crystal from the initial seed crystals. Infrared measurements showed no absorptions due to water, con-

firming that the crystals were free of any water.

For low-temperature spectra, the crystals were mounted on a copper sample block on the bottom of the liquid-helium reservoir of a Hofmann optical Dewar giving a lowest crystal temperature of 15 °K.

The scattered light was dispersed with a Jarrell-Ash model 25-103 1-m double monochromator and detected photoelectrically with a thermoelectrically cooled E.M.I. 6255 SA photomultiplier. In some measurements, a $\frac{1}{3}$-m monochromator was attached to the double monochromator to produce a triple monochromator. This was useful for reducing stray light in cases where the Raman lines were very weak.

In the case of the cobalt chloride crystals, the absorption at all the argon-ion laser frequencies used was sufficiently high to require the use of a surface scattering technique in which the laser light is incident and scattered off the same surface. This technique was also used in obtaining polarization spectra as it has the advantage of requiring only one polished crystal surface, perpendicular to the c axis, giving less depolarization of the incident laser beam.

III. EXPERIMENTAL RESULTS

The Raman spectra of cobalt in the four host crystals were measured for a range of cobalt concentrations. The Raman spectra observed for the three chloride crystals are very similar to each other, while that for the bromide differed in some respects. All the Raman spectra showed two narrow and intense lines due to the Raman active $\vec{k}=0$ phonons of the host lattices.

Raman lines due to electronic transitions of cobalt were identified by their correlation with the cobalt concentration. Raman lines due to two-phonon processes also occur. These have an intensity which is enhanced by the presence of impurities in the crystals. However, they can be distinguished from the cobalt electronic Raman lines by their presence in the same host crystals doped with other ions, such as nickel. Fluorescence lines also occur in some crystals and can be distinguished in the usual way by comparison of the spectra for two different laser excitation frequencies.

The identification of the electronic Raman lines of the single cobalt ions from their cobalt concentration dependence was confirmed by their polarization properties which are consistent with the selection rules for Raman active transitions between the appropriate electronic states (Sec. IV).

The basic similarity of the Raman spectra in all four hosts was helpful in determining the complete spectra in all the crystals. The electronic Raman spectra of cobalt chloride are relatively intense because of the 100% cobalt concentration and this established the pattern of the electronic energy levels.

In the case of the cadmium- and manganese-chloride crystals, the lowest electronic level was obscured by the A_{1g} Raman phonon line.[1] Its position was determined from the frequencies of transitions from it to higher excited levels observed in the room-temperature spectra.

The Raman spectrum of cadmium-chloride crystals containing 5% by weight of chloride is given in Fig. 1. Polarization studies on the lines at 948 and 921 cm^{-1} showed that the 948-cm^{-1} line decreases markedly in the $x(zz)x$ polarization direction while the 921-cm^{-1} line shows little change (Fig. 2). These lines are therefore assigned as transitions to $\gamma_{5,6}^{+}$ and γ_4^{+} symmetry states, respectively (Sec. IV).

The room-temperature spectra have a line at 715±5 cm^{-1} which gives the energy of the lowest electronic level as 235±10 cm^{-1}.

As the cobalt concentration is increased additional Raman lines appear due to the formation of cobalt ion clusters. Figure 3 shows the spectra of crystals containing from 0 to 100 wt% of cobalt chloride and Table I gives the spectral data from the 1000-cm^{-1} region, together with an assignment of the lines due to cobalt pairs of adjacent cobalt ions in the cadmium planes.

The liquid-helium-temperature Raman spectra of cadmium bromide crystals containing 0, 3, 5, and 10 wt% cobalt bromide are given in Fig. 4. These spectra are confused by a multiplicity of impurity activated Raman lines due to second-order phonons and fluorescence lines. The only Raman lines that correlate with the presence of single cobalt ions in the 5-wt% crystals have frequencies of 282, 394, 893, and 995 cm^{-1}. A high resolution spectral scan shows that the 893-cm^{-1} line is a doublet with line components at 889 and 894 cm^{-1}. Polarization studies show that the 889-cm^{-1} line is largely unpolarized, the 894 cm^{-1} line is weak for $x(zz)x$ polarization and the 282-cm^{-1} line is reduced in intensity by 30% for this direction. The 889, 894, and 282 cm^{-1} are, therefore, assigned as transitions to electronic states of γ_4^{+}, $\gamma_{5,6}^{+}$, and $\gamma_{5,6}^{+}$ symmetry, respectively. Depolarization effects due to the imperfect crystal surfaces caused only reduced rather than zero intensity to be observed for the $\gamma_{5,6}^{+}$ levels in the $x(zz)x$ polarization direction. In the 5-wt% crystal lines due to cobalt ion pairs are observed at 268, 439, (903), and 1007 cm^{-1} (Table II).

The spectra of $MnCl_2$(Co) are very similar to those of $CdCl_2$(Co), and are shown in Fig. 5. The

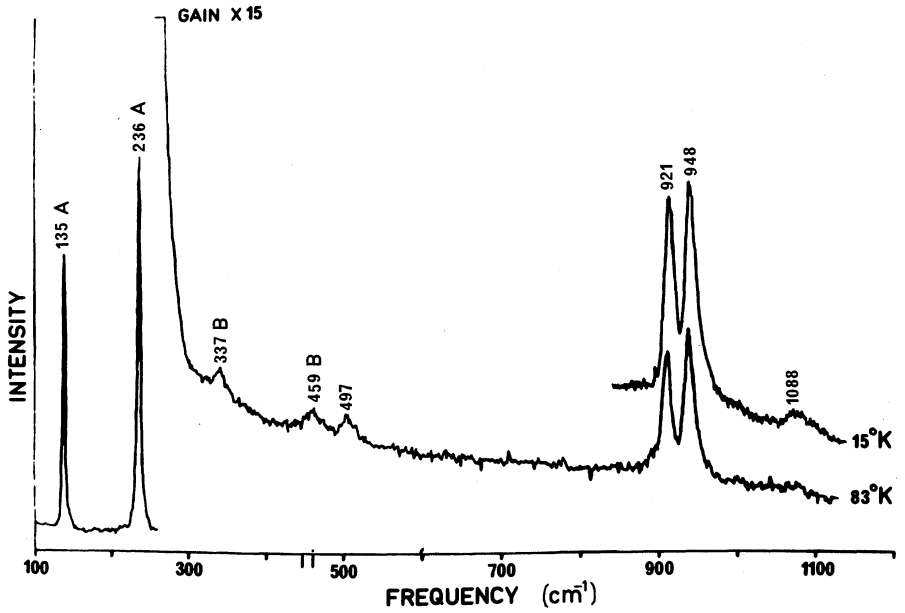

FIG. 1. Raman spectrum of $CdCl_2(Co)$: 5 wt% recorded with spectral slit widths of 1.5 cm^{-1}(100–300 cm^{-1}) and 6.0 cm^{-1} (300–1150 cm^{-1}). First and second-order phonon features are labeled A and B, respectively.

lines are weaker than for the other crystals studied because of absorption of laser light by the pink-colored host crystal and because of the greater width of the lines. For these reasons no attempts were made to determine their polarization. The greater linewidths are attributed to dipolar broadening by the neighboring paramagnetic manganese ions. The room temperature spectra has a line at 745±10 cm^{-1} which indicates the lowest electronic level of the cobalt ion is at 230±13 cm^{-1}.

The room- and liquid-air-temperature spectra of cobalt chloride are shown in Fig. 6; Table III gives the spectral data. At low temperature, there are broad lines at 545 and 978 cm^{-1}, which are asymmetric. The profiles of both of these lines were analyzed by a least-squares-fitting procedure into two overlapping line components for each. Three of these at 549, 963, and 992 cm^{-1} are assigned as electronic transitions of cobalt, while the fourth line, at 522 cm^{-1}, is assigned as a second-order phonon band whose intensity is enhanced by its proximity to the 545 cm^{-1} electronic line. This assignment is supported by the measurements on the antiferromagnetic ordered cobalt chloride crystals below 24.7 °K where the three electronic lines narrow considerably and shift to higher frequencies while the 522 cm^{-1} line becomes a broad weak line centered at 510 cm^{-1} (Fig. 7).

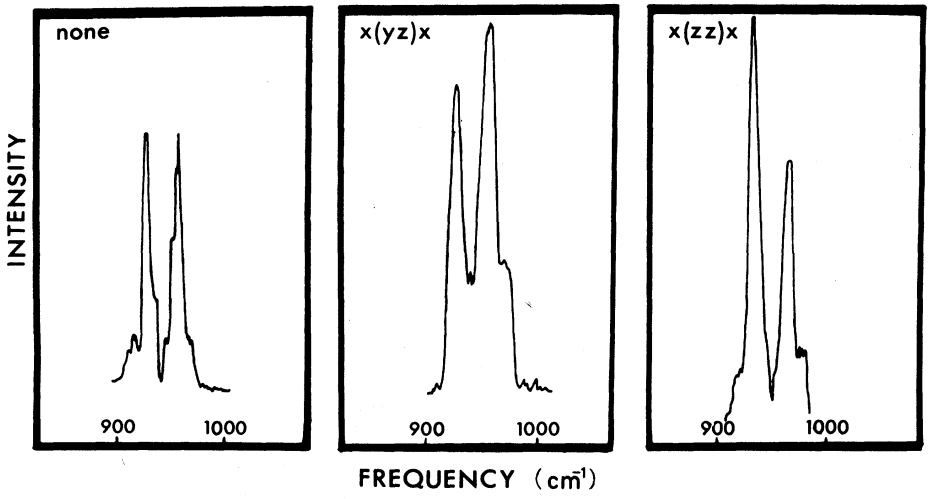

FIG. 2. Polarized Raman spectrum of $CdCl_2(Co)$: 5 wt%, recorded at 78° K (900–1000 cm^{-1}).

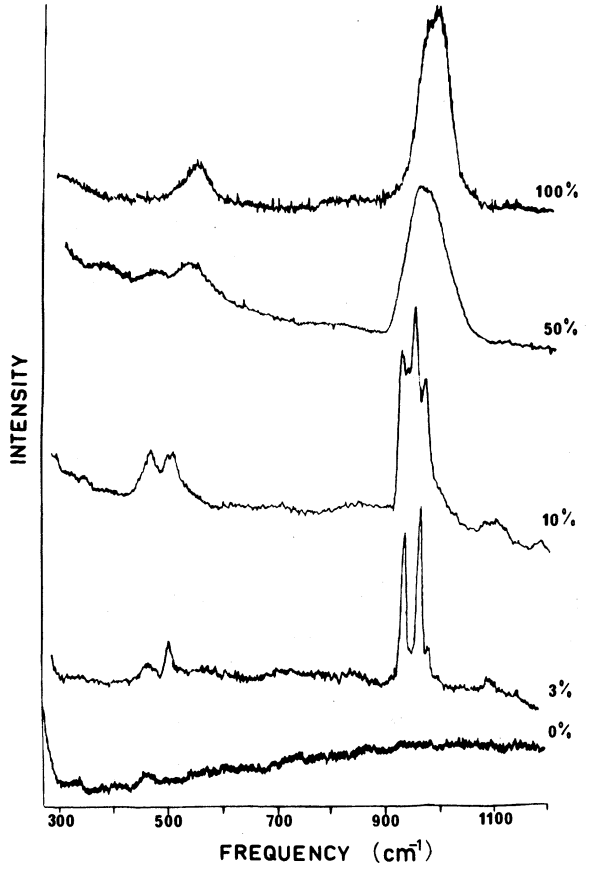

FIG. 3. Raman spectra of $CdCl_2(Co)$: 0, 3, 10, 50, and 100 wt%, all recorded at 15° K, excepting that of the 100% $CoCl_2$ crystal (~30 °K), and with a common spectral width of 6.0 cm^{-1}.

TABLE I. Classification by nearest-neighbor (nn) cation environment of the Co^{2+} electronic lines of $CdCl_2(Co)$, in the 1000-cm^{-1} region.[a]

Number of nn Co^{2+} ions	Co^{2+} concentration 2.5 (wt%)	5.0 (wt%)	10.0 (wt%)	100.0 (wt%)
0	499±2	497±2	495±2	
	923±1	921±1	918±1	
	953±1	948±1	944±1	
	1088±3	1088±2	1088±2	
1	517±1	513±1	508±1	
	937±3		929±1	
	969±2	966±2	961±1	
6				963±4
				992±4

[a] All frequencies in wave numbers (cm^{-1}).

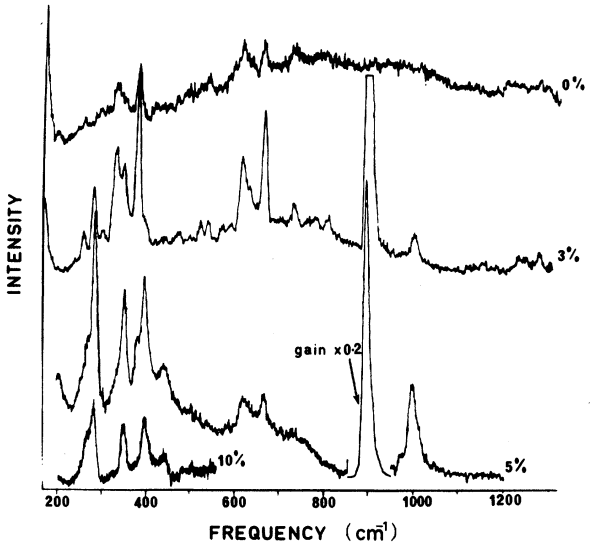

FIG. 4. Raman spectra $CdBr_2(Co)$: 0, 3, 5, and 10 wt%, all recorded at 15 °K with a spectral width of 6.0 cm^{-1}.

Two Raman lines, present only in the room temperature spectrum, occur approximately 220 cm^{-1} below corresponding lines of the low-temperature spectra and confirm the assignment of the line observed at 220 cm^{-1} as the lowest electronic level.

IV. THEORY AND ANALYSIS OF THE SINGLE-ION COBALT SPECTRA

The electronic Raman lines observed comprise transitions between the energy levels of the $3d^7$ configuration and their frequencies and relative intensities are determined by the energy levels and states of this configuration. Because the Raman data give the position of all the energy levels for the lowest cubic crystal-field term of

TABLE II. Frequencies (cm^{-1}) of Raman lines for $CdBr_2(Co)$ crystals of varying cobalt concentration recorded at 15 °K.

Concentration 0 (wt%)	3 (wt%)	5 (wt%)	10 (wt%)
200±1	200±1	~200	•••
	•••	268±2	271±3
	282±1	284±1	286±2
	351±1	351±1	352±2
	394±1	397±1	400±2
	440±2	439±1	444±2
	889±1	(893±1)	887±1
	894±1	unsplit	893±1
	905±1	•••	903±1
	995±1	993±1	unresolved
	•••	1007±2	unresolved

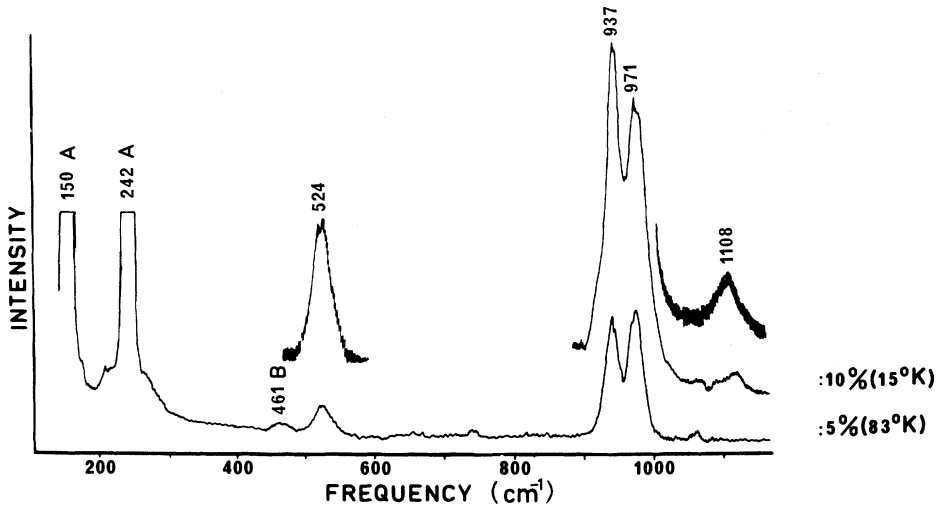

FIG. 5. Raman spectra of $MnCl_2$(Co): 5 and 10 wt%, both recorded with a spectral width of 6.0 cm^{-1}. First and second order phonons are labeled A and B respectively.

cobalt, it is worthwhile to calculate the position of these energy levels of the $3d^7$ configuration for the case of a site of D_{3d} symmetry. Because previous attempts[15] to accurately fit all the observed Raman frequencies were unsuccessful, this calculation was extended to include all 120 states of the $3d^7$ configuration.

The ion arrangement in cadmium-chloride-type crystals has been given by Ono *et al.*[5]; the structure belongs to the D^5_{3d} space group[6] and the cation-site symmetry is D_{3d}. The divalent cobalt ion in these crystals is surrounded by a nearly octahedral arrangement of anions, the octahedron being slightly expanded along one of its trigonal axes. The crystal field is thus predominantly cubic with a small trigonal component giving relatively small splittings of the cubic-field electronic levels. The combined effect of this together with the spin-orbit interaction on the $^4T_{1g}$ (^4F) ground term is to produce a manifold of six Kramers doublet levels with an over-all splitting of 1000 cm^{-1}. These levels have either γ_4^+ or $\gamma_{5,6}^+$ symmetry so only two types of transitions are possible from the γ_4^+ symmetry ground level. Here, the γ_4^+, γ_5^+, and γ_6^+ are particular irreducible representations of the D_{3d} double group. The γ_5^+ and γ_6^+ irreducible representations are complex conjugates and are degenerate in the absence of a magnetic field being labeled $\gamma_{5,6}^+$.

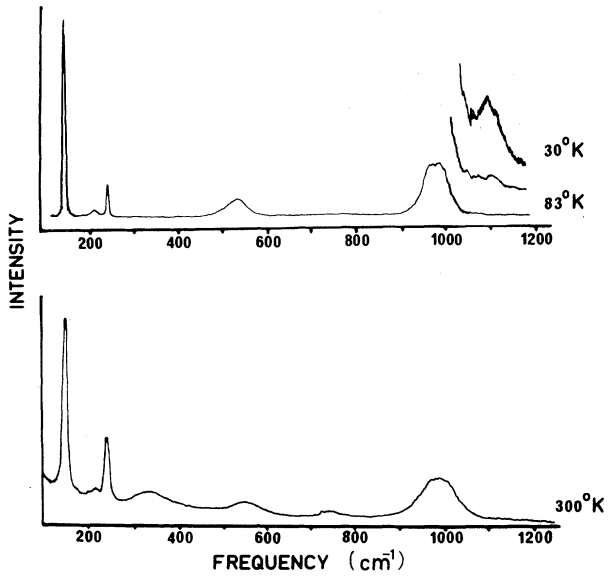

FIG. 6. Raman spectra recorded at 30, 83, and 300° K of $CoCl_2$ in its paramagnetic state.

The selection rules governing the occurrence of Raman active transitions between such levels may be derived from the symmetry properties of the relevant Raman scattering tensors.[7] Thus $\gamma_4^+ \rightarrow \gamma_{5,6}^+$ transitions are absent in $x(zz)x$ polarization while $\gamma_4^+ \rightarrow \gamma_4^+$ transitions occur in all polarizations. The two types of transitions may also be distinguished by comparing the xx and xy polarization spectra, since the xx and xy components in the Raman-scattering efficiency may differ from transitions to γ_4^+ final states but not for transitions to $\gamma_{5,6}^+$ final states.

A. Calculation of the matrix elements of the trigonal crystal field and the Zeeman interaction

For the calculation of the energy levels for divalent cobalt, the strong field approach of Tanabe and Sugano[8] is used.

The energy matrices of the electrostatic interaction and the spin-orbit interaction have already been calculated in the strong-field coupling

TABLE III. Frequencies (cm^{-1}) and widths (cm^{-1}) of observed electronic lines present in the paramagnetic and antiferromagnetic spectrum of $CoCl_2$ in the region 200–1200 cm^{-1}.

Paramagnetic phase						Antiferromagnetic phase	
300 °K		83 °K		~30 °K		15 °K	
Freq	Width	Freq	Width	Freq	Width	Freq	Width
220±5		221±3	20±3	220±3	20±3	233±1	10±1
344±7	75±5						
559±7	70±5	545±5	51±2	549±4	43±1	549±2	20±2
						557±3	28±3
755±7	65±15						
986±9							
				963±4		961.5±1.0	6±1
986±9	90±5	978±7	65±5			983±2	20±3
				992±4	40±1		
						1014±2	18±3
		1115±5	40±10	1115±5	•••	1150±5	30±5

scheme for the $3d^3$ configuration by Sugano[9] and Schroeder,[10] respectively. The electrostatic interaction is expressed in terms of two parameters B and C while the spin-orbit interaction is characterized by parameters ζ and ζ'.[10] We thus only need to calculate the energy matrices for the trigonal crystal field and for the Zeeman interaction in the strong-field coupling scheme to obtain both the position of the energy levels and their g factors for divalent cobalt ions in this symmetry crystal field.

The operator for the trigonal field interaction is developed from the d^1 electron case. It is of T_2 symmetry and has the form

$$V(T_2) = (1/\sqrt{3})(V_\xi + V_\eta + V_\zeta) ,$$

where the V_ξ, V_η, and V_ζ transform like the $\eta\zeta$, $\xi\zeta$, and $\xi\eta$ basis functions of the cubic T_2 irreducible representation, where ξ, η, ζ are the cubic axes.

The trigonal field is described by two trigonal crystal-field parameters, v and v', which are defined in terms of the single-d-electron reduced matrix elements by

$$v = (1/\sqrt{2})\langle t_2 \| V(T_2) \| t_2 \rangle ,$$

$$v' = (1/\sqrt{6})\langle t_2 \| V(T_2) \| e \rangle .$$

The numerical factors in these definitions were chosen to make these parameters identical to those defined by Pryce and Runciman.[11]

The Zeeman operator $(kL + 2S)$ has T_1 symmetry and the z and x components of the orbital part (kL) are expressed in terms of the operators V_α, V_β,

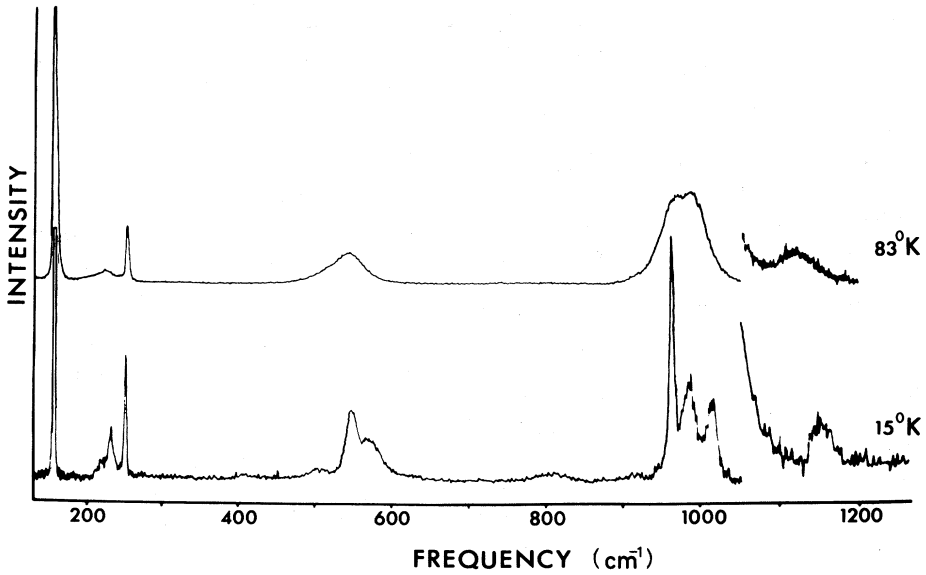

FIG. 7. Raman spectra of $CoCl_2$ in its paramagnetic (T = 83° K) and antiferromagnetic (T = 15° K) states. The latter is constructed from several part spectra as follows: 130–270 cm^{-1} using the 4880-Å laser line and a spectral slit width of 1.5 cm^{-1}; 270–460 cm^{-1}, 4579 Å and 3 cm^{-1}; 460–650 cm^{-1}, 4579 Å and 6 cm^{-1}; 650–900 cm^{-1}, 4765 Å and 6 cm^{-1}; 900–1050 cm^{-1}, 4880 Å and 1.5 cm^{-1}; 1050–1270 cm^{-1}, 4880 Å and 10.5 cm^{-1}.

V_γ which transform like the α, β, γ basis functions of the cubic T_1 representation by

$$V_z(T_1) = (1/\sqrt{3})(V_\alpha + V_\beta + V_\gamma),$$

$$V_x(T_1) = (1/\sqrt{6})(V_\alpha + V_\beta - 2V_\gamma).$$

The two orbital angular momentum reduction factor parameters k and k' are defined by

$$\sqrt{6}\, ik = \langle t_2 \| V(T_1) \| t_2 \rangle ,$$

$$-2\sqrt{3}\, ik' = \langle t_2 \| V(T_1) \| e \rangle ,$$

which are related to those of the spin-orbit interaction by

$$k = \zeta/\zeta_0, \quad k' = \zeta'/\zeta_0 ,$$

where ζ_0 is the free-ion spin-orbit coupling constant. The appropriate S_x and S_z components of the spin operator are similarly expressed and their matrix elements can be evaluated with no additional parameters.

There are 120 states in the $d^3(d^7)$ configuration and matrix elements of the trigonal crystal field and Zeeman interaction are required between all of these.

Since there are no nonzero matrix elements of either the trigonal crystal field or the z component of the Zeeman interaction between γ_4^+ and $\gamma_{5,6}^+$ states, the 120-dimension energy matrices for these interactions can be reduced to two matrices of dimensions 78 and 42, respectively, by using basis states having either γ_4^+ or $\gamma_{5,6}^+$ symmetry. However, the basis states used for the published calculations of the cubic-field, electrostatic, and spin-orbit interaction transform as the irreducible representations of the cubic double group referred to a cubic system of axes, while the γ_4^+ and $\gamma_{5,6}^+$ states appropriate for the site of D_{3d} symmetry refer to a trigonal system of axes, with the principal axis along the diagonal (111) direction of the set of cubic axes. A rotation of the double cubic group basis states was therefore performed to obtain basis states of γ_4^+ or $\gamma_{5,6}^+$ symmetry referred to the trigonal system of axes. The appropriate transformation coefficients were derived from the rotation matrices for the $S = \frac{1}{2}$ and $S = \frac{3}{2}$ spin functions. With these basis states the γ_4^+ matrices of the trigonal crystal field and the z component of the Zeeman interaction simplify further into two 39-dimension matrices corresponding to the two components of the γ_4^+ states.

The x component of the Zeeman interaction has nonzero matrix elements between γ_4^+ and $\gamma_{5,6}^+$ states and it is necessary to diagonalize the full 120-dimension energy matrix for this interaction.

The complete matrices of the trigonal crystal field and the Zeeman interaction are available on request. The reduced matrix elements of $V(T_2)$ and $V(T_1)$ for t_2^3 and t^2e configurations have already been published by Sugano and Peter.[12] All matrices were checked to within a phase by numerical diagonalization. Checks were made by comparison of the eigenvalues with the results for MgO:Cr^{3+} and Al_2O_3:Cr^{3+} obtained by Macfarlane[13] using his weak-field d^3 (d^7) matrices.

B. Fitting of the experimental data

With the implicit assumption of a pure $3d^7$ electron configuration there are seven parameters to determine all the energy levels for a trigonal symmetry site. These are the cubic crystal-field parameter $\Delta(=10Dq)$, the two electrostatic parameters B and C, the two trigonal crystal-field parameters v and v' and the two spin-orbit parameters ζ and ζ'. The five observed electronic Raman lines are transitions between the six spin-orbit and trigonal crystal-field levels of the $^4T_{1g}(^4F)$ cubic crystal-field term, and, therefore, do not depend on the values for the cubic crystal field or the electrostatic parameters. These were set at the values obtained from the cubic crystal field analysis of the optical spectra of cobalt chloride and of cadmium chloride and bromide containing cobalt carried out by Ferguson *et al.*[14] and Robson.[15] The values appropriate to manganese chloride containing cobalt were taken as the same as those for cobalt chloride, since these two crystals have closely similar dimensions.

The frequencies of the electronic Raman lines were then fitted by an iterative least-squares routine by adjusting the four parameters ζ, ζ', v, v'. The results are given in Table IV.

In the case of cadmium-chloride and -bromide crystals the g values for the ground state level are known from EPR measurements[16,17] and the set of parameters obtained could be tested by comparing these g values with the calculated splitting factors for the ground-state level for these parameters. These are shown in Table V.

The least-squares routine was modified to include the deviation of the observed value for $g_\parallel$ from the calculated one. This was done in the expectation that only slight adjustments in the parameter values may allow exact fit of the observed g values without degrading significantly the energy-level fit. No new parameters need to be introduced because the parameters k and k' characterizing the z component of the Zeeman interaction are related to the spin-orbit interaction parameters ζ and ζ' (Sec. IV A).

The corresponding $g_\perp$ deviation was not included because it would necessitate diagonalizing the whole 120-dimension matrix. The $g_\parallel$ deviation was weighted heavily to take account of the greater experimental precision in its value.

TABLE IV. Calculated and observed energies of the six Kramers degenerate electronic lines of the $^4T_{1g}(^4F)$ term.[a]

Assignment	$CdBr_2$(Co) : 3 (wt%) Expt	Calc	$CdCl_2$(Co) : 2.5 (wt%) Expt	Calc	$MnCl_2$(Co) : 5 (wt%) Expt	Calc	$CoCl_2$ Expt	Calc
$\gamma_5^+ + \gamma_6^+(^{(1)}\Gamma 8^+)$	282±1	282	235±10	225	230±13	217	220±3	217
$\gamma_4^+(^{(1)}\Gamma 8^+)$	394±1	394	499±2	497	524±3	522	549±4	546
$\gamma_4^+(^{(2)}\Gamma 8^+)$	889±1	889	923±1	923	938±2	939	963±4	965
$\gamma_5^+ + \gamma_6^+(^{(2)}\Gamma 8^+)$	894±1	894	953±1	953	972±2	972	992±4	991
$\gamma_4^+(\Gamma 7^+)$	995±1	995	1088±3	1091	1108±3	1108	1115±5	1115
Parameters of energy matrix								
Dq	−610		−670		−690		−690	
B	790		790		780		780	
C	3090		3320		3432		3432	
ζ	−544		−512		−516		−533	
ζ'	−432		−513		−515		−503	
v	129		57		124		440	
v'	−227		−345		−433		−694	

[a] All measurements and parameters in units of wave numbers (cm^{-1}).

For $CdCl_2$:Co^{2+}, the g-value fit was found to be very good and it did not prove possible to improve the agreement without destroying the energy-level fit.

For $CdBr_2$:Co^{2+}, the experimentally observed g values were very different from those calculated and it was not possible to find any set of parameters that would bring the calculated values close to the experimental values. To resolve this discrepancy, the EPR measurements on this crystal (0.1 wt%) were repeated for us by Edgar,[18] with the results given in Table V, which show the previous EPR results are in error.

The inclusion of the $g_\parallel$ deviation into the least squares routine did not result in a significantly better fitting. In both $CdCl_2$:Co^{2+} and $CdBr_2$:Co^{2+} this is due to the relative insensitivity of the g values to small parameter variations about the optimum set obtained from the energy fit above. The final energy-level fit obtained is within the experimental accuracy of measurement of the observed lines, while the g values are fitted to with 0.15.

TABLE V. Calculated and observed g values for the $(\Gamma_6^+)\ \gamma_4^+$ $CdCl_2 : Co^{2+}$ and $CdBr_2 : Co^{2+}$ crystals.

	$CdBr_2 : Co^{2+}$ Expt	Calc	$CdCl_2 : Co^{2+}$ Expt	Calc
$g_\parallel$	3.74±0.1[a]	3.59	3.06±0.05[a]	3.02
	2.71±0.05[b]		3.06±0.02[b]	
			3.04±0.02[c]	
$g_\perp$	4.67±0.1[a]	4.66	4.96±0.05[a]	5.07
	4.99±0.05[b]		4.98±0.02[b]	
			4.95±0.02[c]	

[a] A. Edgar (Ref. 18).
[b] K. Morigaki (Ref. 16).
[c] J. W. Orton (Ref. 17).

Previous calculations[15,19] of the spin orbit and trigonal crystal-field energy levels of the $^4T_{1g}(^4F)$ cubic-field ground-state multiplet have allowed an admixture of the levels of the $^4T_{1g}(^4P)$ term and yield an energy-level scheme which approximates that obtained here using all the states of the $d^3(d^7)$ configuration (Fig. 8). The principal difference is in the splitting of the upper levels in the more exact calculation. The absence of such splitting in the earlier calculations prevented a good energy-level fit to the observed levels.

Allowance was made for this splitting in the calculation of the energy levels of cobalt chloride by Hsu and Stout,[20] although only states from the $^4T_{1g}(^4F)$ and $^4T_{1g}(^4P)$ terms were included in their analysis.

The exact values obtained for the trigonal field parameters are not physically significant because of the sensitivity of these parameters to the experimental accuracy of the data. It was found that relative variations of a few cm^{-1} in the measured energy levels could alter the parameters by 15%. In comparison, the spin-orbit parameters were insensitive to such changes. In view of this, further refinements in the fit by remeasuring the optical absorption spectra of each crystal in greater detail and refitting the cubic field and electrostatic parameters is not justified.

The values obtained for the two spin orbit parameters are closely equal in the case of the chloride and the data could have been fitted equally well using one spin-orbit parameter, as is usually done in the weak-field calculations.[21] On the other hand, the data for the bromide requires distinctly different values for the two parameters and it is not possible to obtain a good energy level and g-

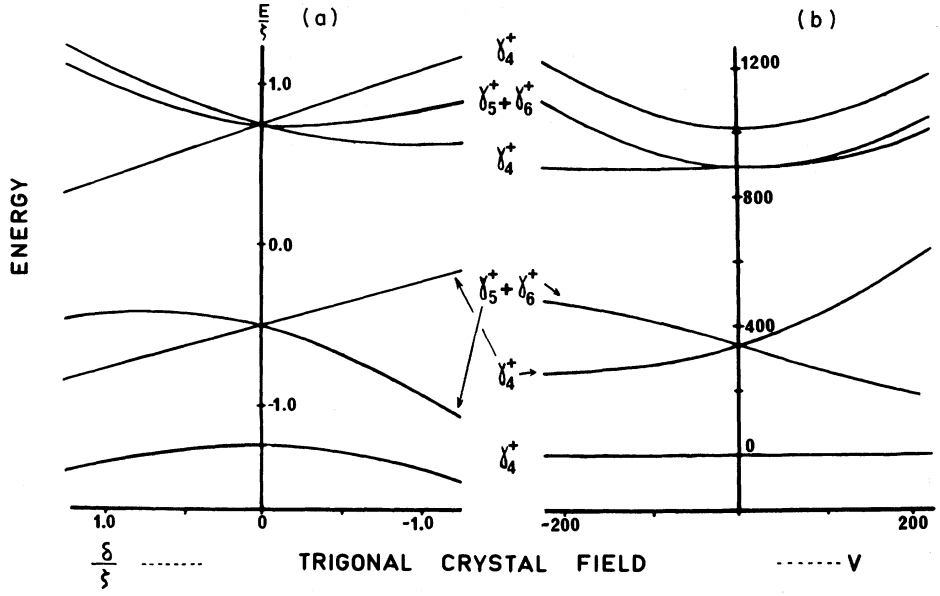

FIG. 8. Energy-level calculations for Co^{2+} in a trigonal crystal field: (a) Robson's calculation (Ref. 15) (δ and ζ are the trigonal and spin-orbit parameters, respectively). (b) The full $3d^3$ calculation for $Dq = -690$, $B = 780$, $C = 3432$; spin-orbit parameters; $\zeta = -510$, $\zeta' = -540$ (all cm^{-1}); trigonal parameters $v/v' = -0.323$.

value shift if the two parameters are set to the same value.

In all cases, the spin-orbit parameter values are close to the free-ion spin-orbit coupling constant $\zeta_0 = -535$ cm^{-1} and there is little covalency reduction. This may be expected from the intraconfigurational nature of the transitions which are all between states of the $t_{2g}^5 e_g^2$ configuration.

The trigonal-field parameters are similar for all the chloride crystals, and differ in the case of the bromide. Their d^3 configuration values are characterized by a positive v and a negative v' with $v'/v \approx -3$. Their magnitudes are small compared to those usually obtained for trigonally distorted crystals[13] consistent with the small trigonal distortion of the cadmium chloride lattice.

The electrostatic contributions to the trigonal crystal field in cadmium-chloride-type crystals come from the small departure from cubic symmetry of the octahedron of nearest-neighbor chlorine ions, the noncubic arrangement of the next-nearest-neighbor cadmium ions, and the electric dipole moments induced on the chlorine ions, by the cadmium ions.[22] The main part of the trigonal crystal field comes from the noncubic arrangement of the cadmium ions and the induced chlorine dipole moments. Kanamori[22] calculated the trigonal crystal field for cobalt chloride due to these two contributions and found the contribution due to the noncubic arrangement of the cadmium ions was sufficient to split the $^4T_{1g}(^4F)$ term into two levels, $^4A_{1g} + {}^4E_g$, separated by 1000 cm^{-1}. Inclusion of the contribution from the chloride dipole moments modified this energy-level separation and for large induced dipole moments, the level scheme was reversed. A calculated splitting of 1000 cm^{-1} is large compared to that actually observed hence these electrostatic contributions can more than account for the magnitude of the trigonal crystal-field parameters obtained from the analysis of the spectra. A quantitative calculation is not possible at present as it would require knowledge of the magnitude of the induced dipole moments on the chlorine ions and the inclusion of the effects of covalency, overlap, and other nonelectrostatic contributions.

V. MOLECULAR-FIELD ANALYSIS OF THE COBALT-CHLORIDE SPECTRA BELOW 25°K

The Raman spectra of cobalt chloride below 24.71°K show splitting of the single ion levels due to exchange interactions between the cobalt ions. In view of the calculation of Hsu and Stout,[20] it is worthwhile attempting a revised calculation to fit the additional levels observed. The molecular-field interaction perpendicular to the c axis is represented by

$$H = -2J_{\text{eff}}(S_x)_0 S_x ,$$

where $(S_x)_0$ is the expectation value of S_x for the ground state of the cobalt ion, and J_{eff} is the effective exchange interaction which includes the effect of both intra- and inter-layer exchange interactions. The energies of the twelve exchange split levels of the $^4T_{1g}(^4F)$ term are obtained by diagonalizing the dimension-12 matrices for this interaction, using as basis states the twelve lowest levels obtained by diagonalizing the full 120-dimension free-ion and crystal-field matrices of

$3d^7$ configuration.

For $2J_{eff} = 16\ cm^{-1}$, the energy levels given in Fig. 9 are obtained and are in good agreement with experimentally observed transitions. However, the transition to the lowest-lying energy level is calculated to be $30\ cm^{-1}$, whereas this level has been observed to occur at $19.2\ cm^{-1}$ by Jacobs *et al.*[23] This discrepancy can be attributed to the use of an exchange interaction Hamiltonian appropriate for an $S = \frac{1}{2}$ level for calculating the energies of the levels of a $^4T_1$ orbital triplet.

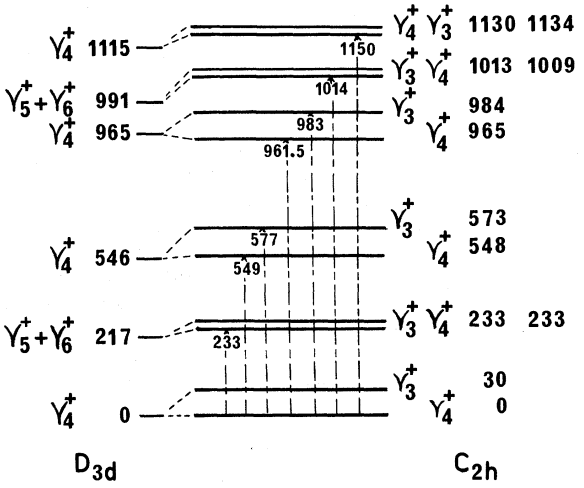

FIG. 9. Calculated and observed energy levels (cm^{-1}) within the ground $^4T_{1g}(^4F)$ term of a Co^{2+} ion in both a purely trigonal and trigonal plus exchange field (Table III).

VI. SUMMARY

All the trigonal crystal-field energy levels of the lowest cubic-field multiplet of cobalt have been determined and fitted exactly with a crystal-field model which includes all states of the $3d^7$ configuration. Good agreement is also obtained with the known ground-state g factors. Zeeman Raman experiments could verify the parameter fits obtained.

ACKNOWLEDGMENTS

This work was supported by the N. Z. University Grants Committee through the award of postgraduate scholarships to two of the authors (J. H. Christie and I. W. Johnstone). The authors are grateful to Dr. R. W. G. Syme for helpful discussions, to R. Ritchie for growing crystals, to R. W. Tyree for technical assistance, and to Professor B. G. Wybourne for his interest and support.

*Work done in partial fulfilment of the requirements for the Ph.D. dissertations of J. C. Christie and I. W. Johnstone.

†Present address: Institute of Radio Engineering and Electronics, Czechoslovakia Academy of Science, Prague 18088, Czechoslovakia.

[1]D. J. Lockwood, J. Opt. Soc. Am. 63, 374 (1973).

[2]J. H. Christie and D. J. Lockwood, in *Light Scattering in Solids*, edited by M. Balkanski (Flammarion, Paris, 1971), p. 145.

[3]J. H. Christie and D. J. Lockwood, Chem. Phys. Lett. 8, 120 (1971).

[4]J. H. Christie and D. J. Lockwood, Chem. Phys. Lett. 9, 559 (1971).

[5]K. Ono, A. Ito, and T. Fujita, J. Phys. Soc. Jpn. 19, 2119 (1964).

[6]R. W. G. Wyckoff, *Crystal Structures*, 2nd ed. (Wiley, New York, 1964), Vol. 1, Chap. 4, p. 270.

[7]R. Loudon, Adv. Phys. 13, 423 (1964).

[8]S. Sugano, Y. Tanabe, and H. Kamimura, *Multiplets of Transition-Metal Ions in Crystals* (Academic, New York, 1970), Appendix II, p. 286.

[9]Y. Tanabe and S. Sugano, J. Phys. Soc. Jpn. 9, 753 (1954).

[10]W. A. Runciman and K. A. Schroeder, Proc. R. Soc. A 265, 489 (1962).

[11]M. H. L. Pryce and W. A. Runciman, Discuss. Faraday Soc. 26, 34 (1958).

[12]S. Sugano and M. Peter, Phys. Rev. 122, 381 (1961).

[13]R. M. Macfarlane, Phys. Rev. B 1, 989 (1970).

[14]J. Ferguson, D. L. Wood, and K. Knox, J. Chem. Phys. 39, 881 (1963).

[15]A. B. Robson, M. Sc. thesis (University of Canterbury, 1969) (unpublished).

[16]K. Morigaki, J. Phys. Soc. Jpn. 16, 1639 (1961).

[17]J. W. Orton, Rept. Prog. Phys. 22, 204 (1959).

[18]A. Edgar (private communication).

[19]M. E. Lines, Phys. Rev. 137, A982 (1965).

[20]E. C. Hsu and J. W. Stout, J. Chem. Phys. 59, 502 (1973).

[21]R. M. Macfarlane, J. Chem. Phys. 39, 3118 (1963).

[22]J. Kanamori, Prog. Theor. Phys. Jpn. 20, 890 (1958).

[23]I. S. Jacobs, S. Roberts, and S. D. Silverstein, J. Appl. Phys. 39, 816 (1968).